Electronic Supplementary Material (ESI) for Journal of Materials Chemistry A
This journal is © Royal Society of Chemistry 2018

Supplementary Information

New Reflowing Strategy Based on Lithiophilic Substrate towards Smooth and Stable Lithium Metal Anode

Rensheng Song[a], Yuqiang Ge[b], Bo Wang[a,*], Qiang Lv [a], Fei Wang[a], Tingting Ruan[a], Dianlong Wang[a,*], Shixue Dou[c], Huakun Liu[c]

[a] *MIIT Key Laboratory of Critical Materials Technology for New Energy Conversion and Storage, School of Chemistry and Chemical Engineering, Harbin Institute of Technology, 150001 Harbin, China.*
[b] *State Key Laboratory of Advanced Welding and Joining, Harbin Institute of Technology, Harbin 150001, China.*
[c] *Institute for Superconducting & Electronic Materials, Australian Institute of Innovative Materials, University of Wollongong, Wollongong, NSW 2500, Australia.*

∗ Corresponding author. Fax: +86 45186413721; Tel: +86 45186413751.
E-mail address:
wangbo19880804@163.com (B. Wang),
wangdianlonghit@163.com (D. L. Wang)

Figures

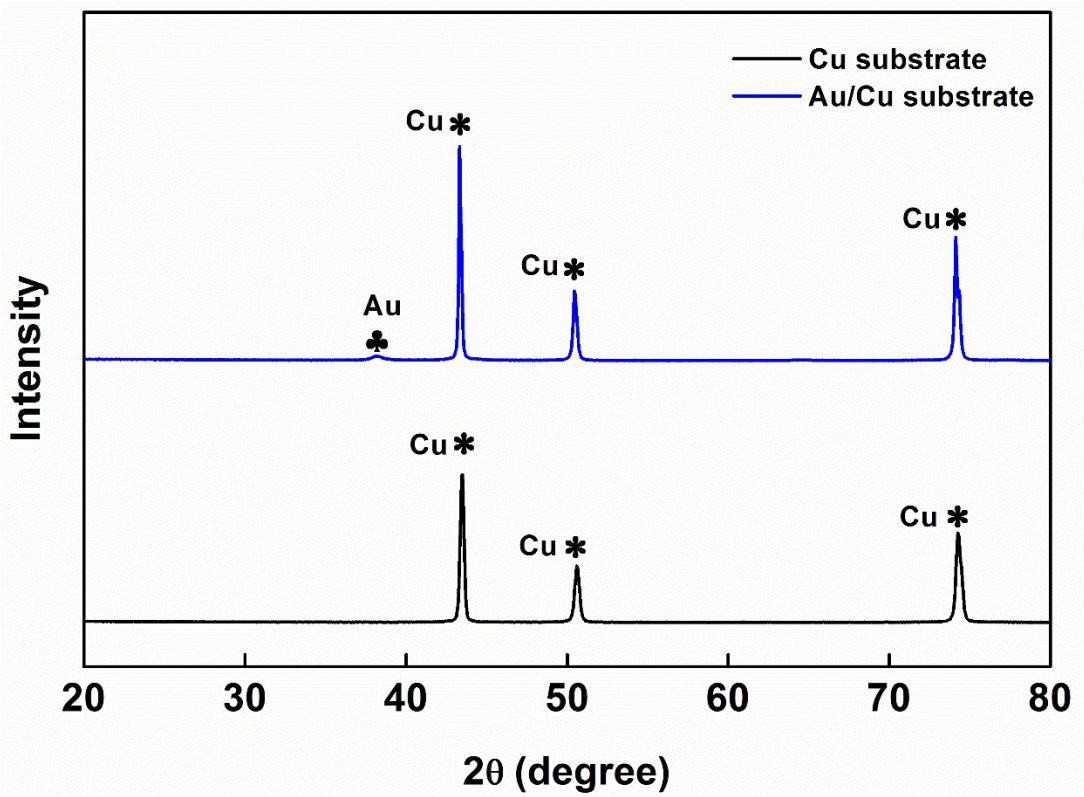

Fig. S1† XRD patterns of Cu and Au/Cu substrates.

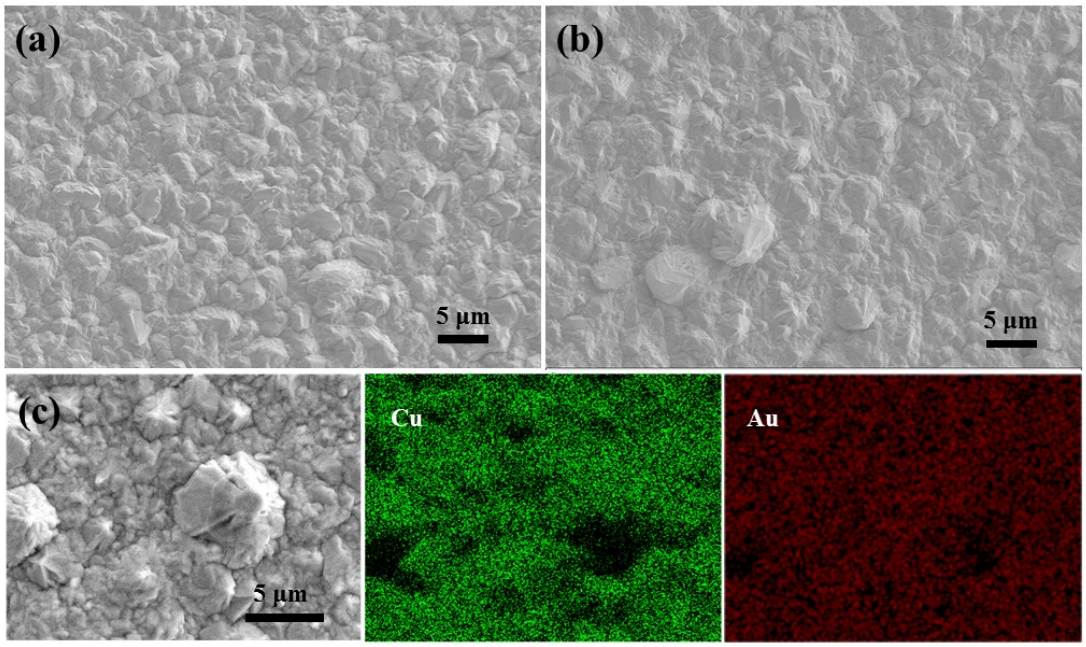

Fig. S2† SEM images of (a) Cu and (b) Au/Cu substrates. (c) The energy dispersive X-ray spectrometer (EDS) mapping for the distribution of carbon and golden elements on the surface of Au/Cu substrate.

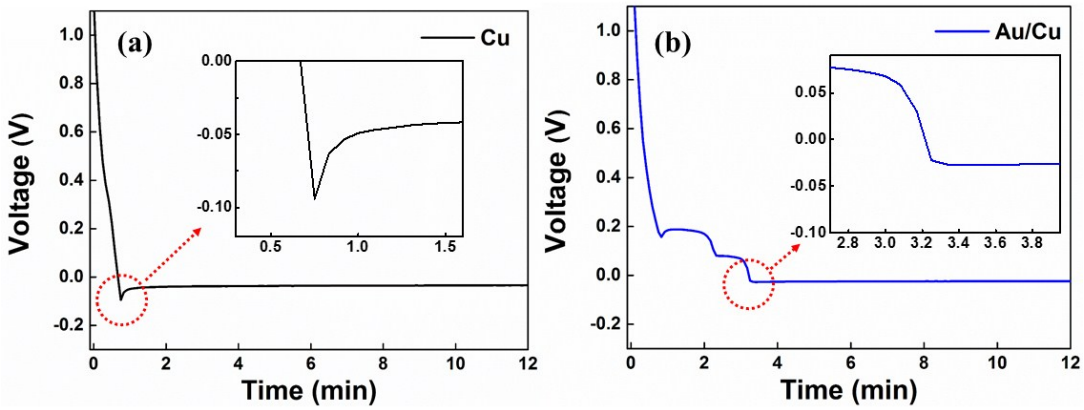

Fig. S3† Voltage profiles during initial Li deposition at 0.5 mA cm^{-2} onto a) Cu and b) Au/Cu substrates. Insets in (a) and (b) are the corresponding magnified images.

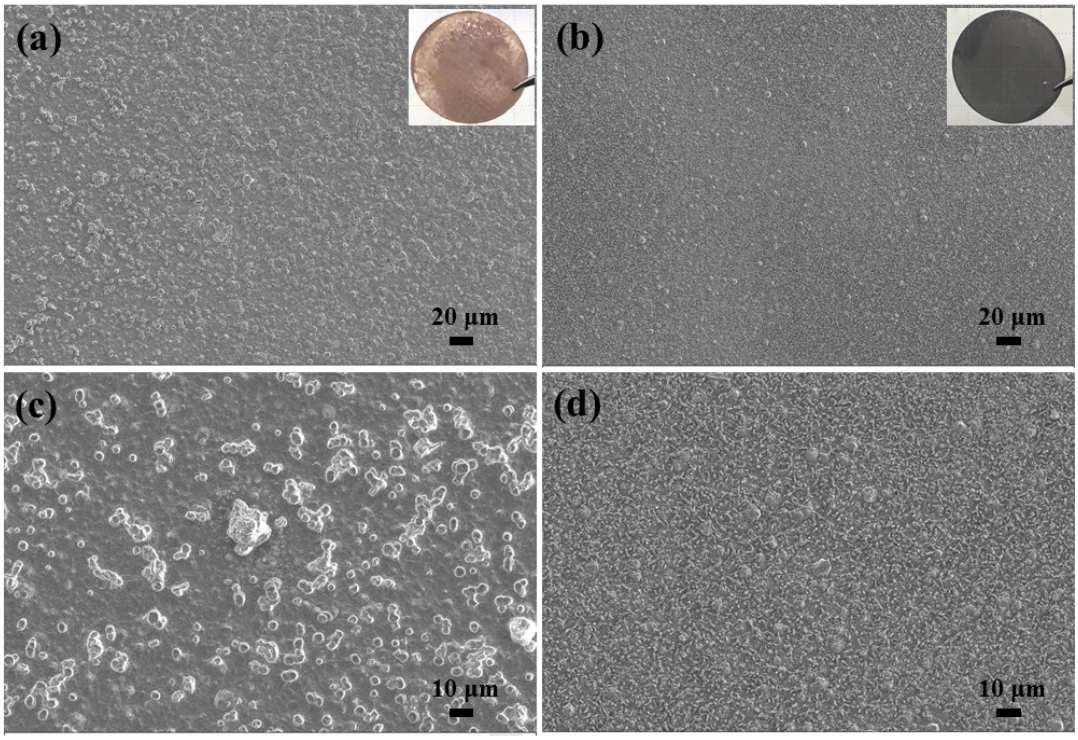

Fig. S4† SEM images of (a, c) Cu and (b, d) Au/Cu substrates with 0.1 mAh cm^{-2} Li deposition under the current density of 0.5 mA cm^{-2}. Insets are their corresponding digital photographs, with each electrode having the diameter of 14 mm.

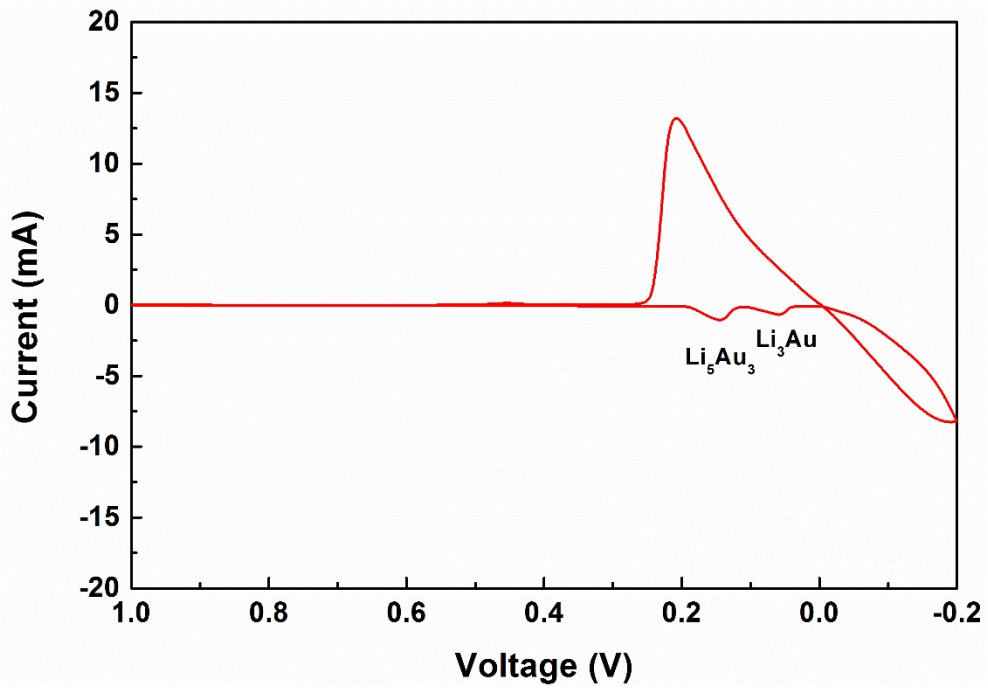

Fig. S5† The CV measurements of the half cell with Au/Cu electrode were conducted with a potential window from +1V to -0.2 V at a scan rate of 0.5 mV s^{-1}.

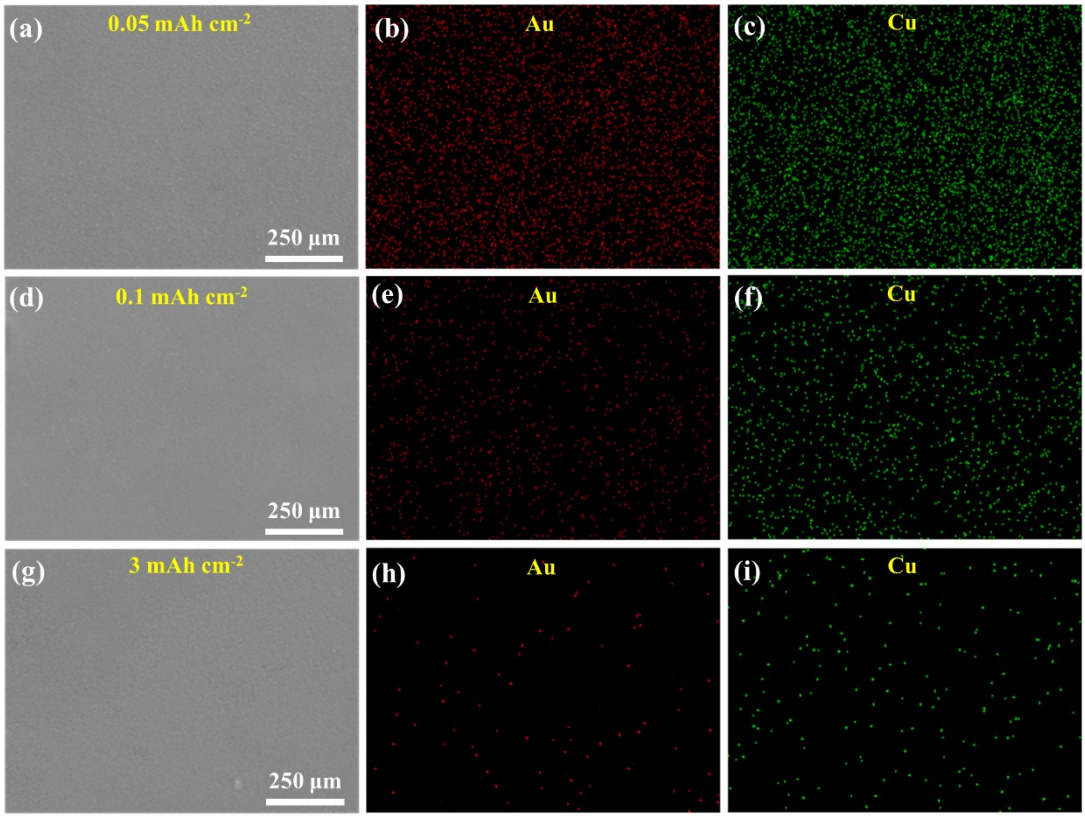

Fig. S6† The EDS mapping result of Au and Cu elements on the surface of Li/Au/Cu electrode with Li plating capacities of (a-c) 0.05, (d-f) 0.1, and (g-i) 3 mAh cm^{-2}, respectively.

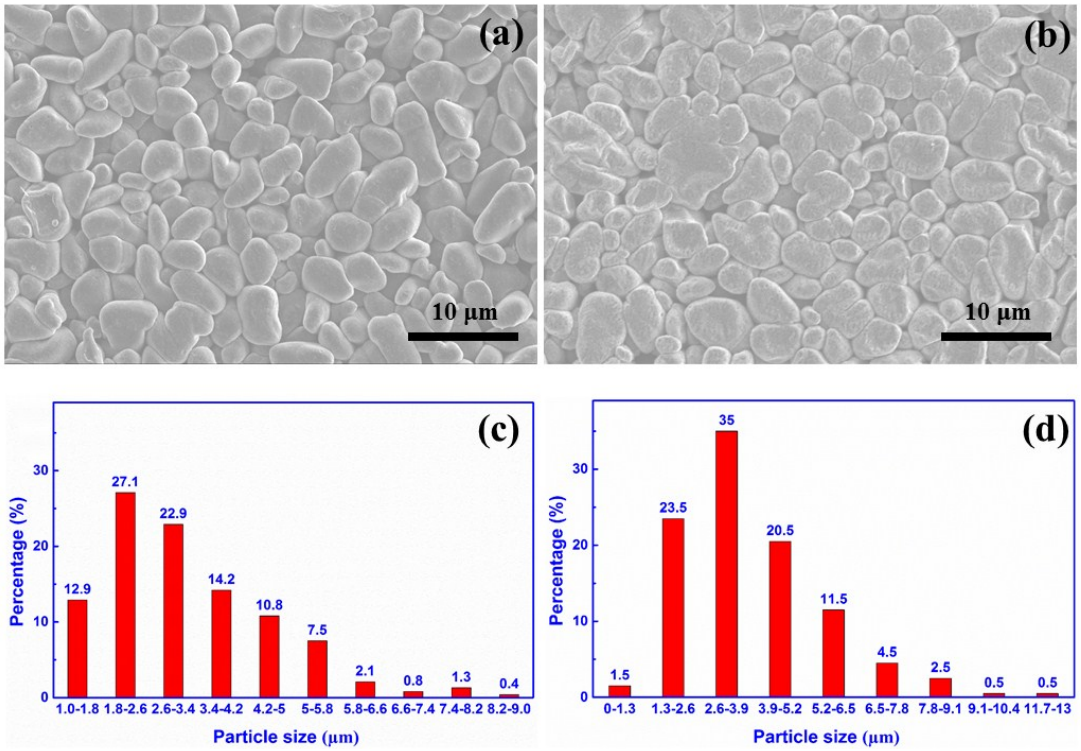

Fig. S7† SEM images of (a) untreated Li/Au/Cu and (b) RF-Li/Au/Cu electrodes with low magnification. The particle size distribution of (c) untreated Li/Au/Cu and (d) RF-Li/Au/Cu electrodes was measured by Nano Measure software. For untreated Li/Au/Cu electrode, there are 40% of particles whose size is below 2.6 nm, indicating there is a large number of small particles. In contrast, there is only 25% of particles for RF-Li/Au/Cu electrode whose size is below 2.6 nm. On the other hand, RF-Li/Au/Cu electrode also has more particles with diameters > 5 nm (more than 19.5%) than that of untreated Li/Au/Cu electrode (only 12.1%).

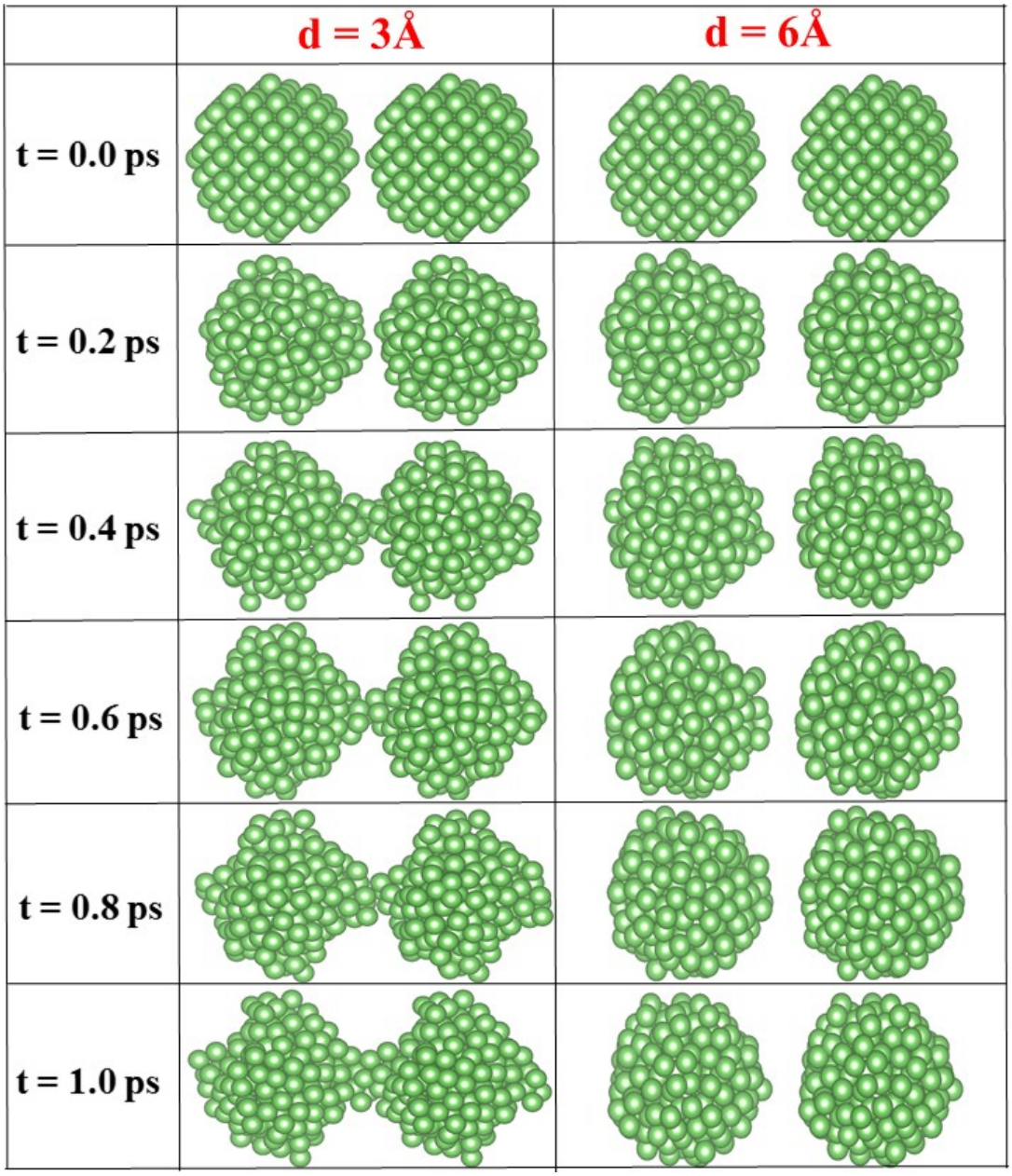

Fig. S8† The evolution processes of Li diffusion for d=3Å and d=6 Å models using the Ab-initio molecular dynamics siluations. For d=3Å model, there is a tendency that Li particles diffuse into together after 0.4 ps, while those of d=6Å model still in a seperate state after 1.0 ps.

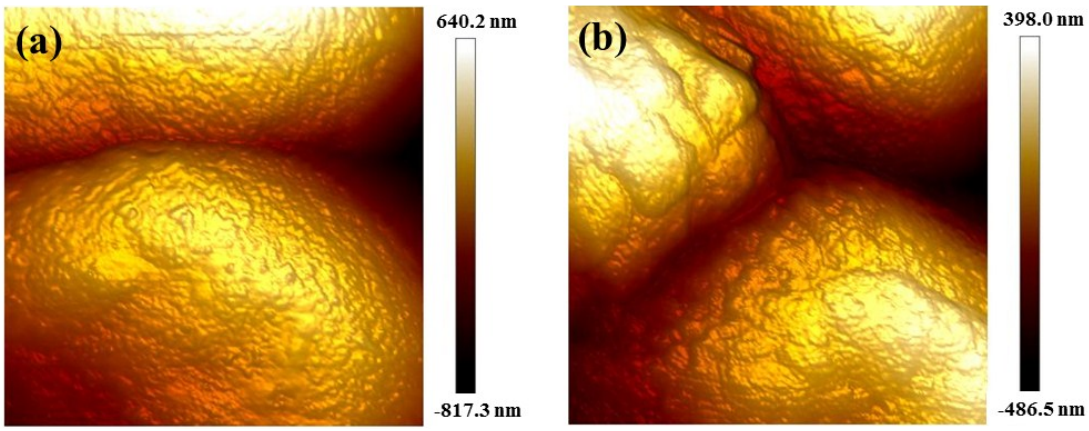

Fig. S9† 2D AFM height images of (a) untreated Li/Au/Cu and (b) RF-Li/Au/Cu electrodes.

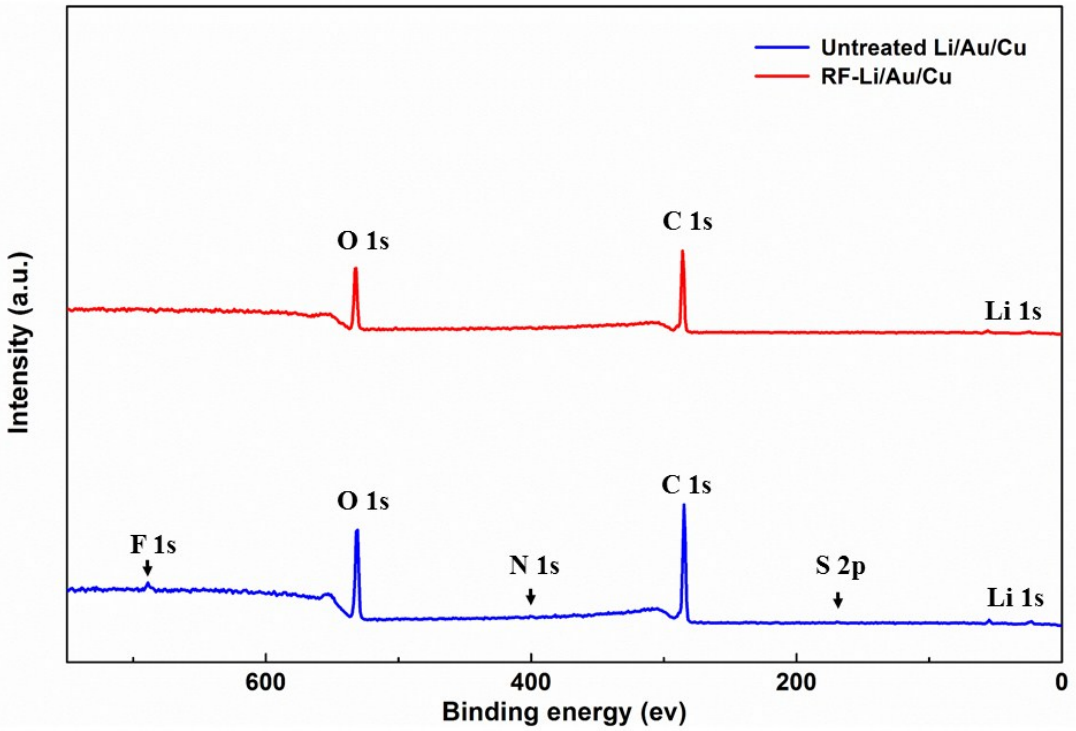

Fig. S10† XPS characterization of the untreated Li/Au/Cu and RF-Li/Au/Cu electrodes.

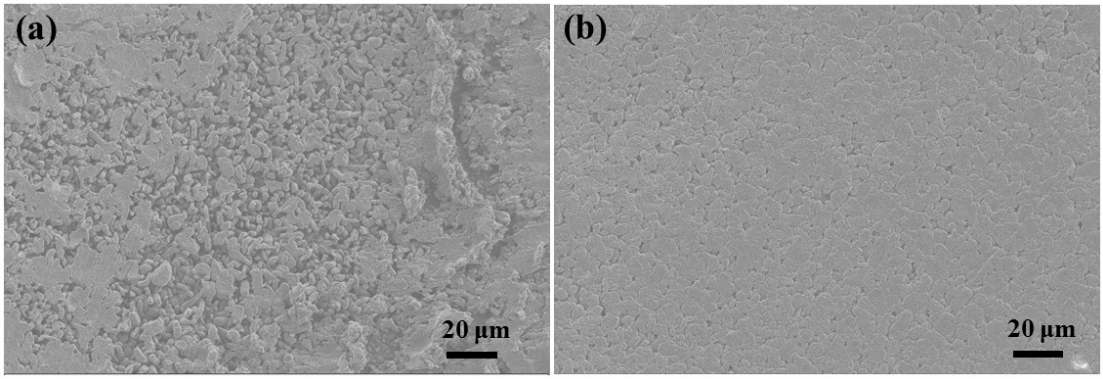

Fig. S11† The low-magnification SEM images of (a) untreated Li/Au/Cu and (b) RF-Li/Au/Cu electrodes after the 10th Li plating with a current density of 1 mA cm^{-2}.

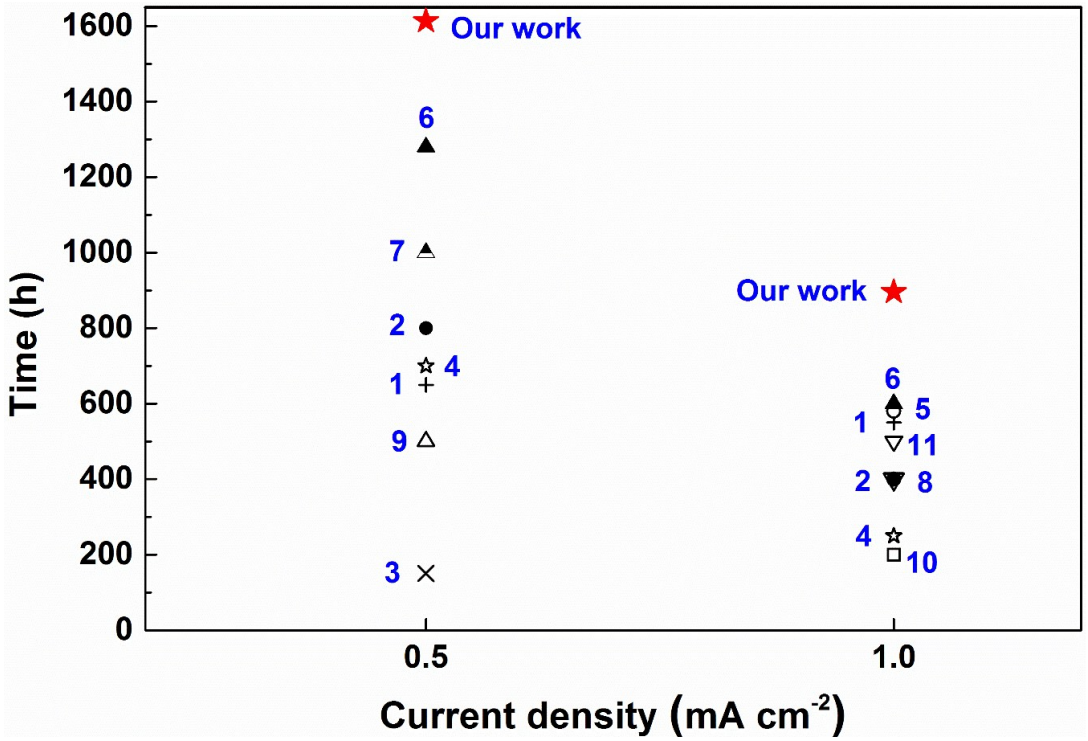

Fig. S12† Comparision of cycling performance of our data and the results reported by other groups under the current density of 0.5 mA cm^{-2} or 1 mA cm^{-2} with a capacity of 1 mAh cm^{-2}.

References

1 S. J. Zhang, Z. G. Gao, W. W. Wang, Y. Q. Lu, Y. P. Deng, J. H. You, J. T. Li, Y. Zhou, L. Huang, X. D. Zhou, S. G. Sun, *Small,* 2018, 1801054.

2 F. Q. Liu, W. P. Wang, Y. X. Yin, S. F. Zhang, J. L. Shi, L. Wang, X. D. Zhang, Y. Zheng, J. J. Zhou, L. Li, Y. G. Guo, *Sci. Adv.*, 2018, **4**, eaat5383.

3 Y. Gao, Y. Zhao, Y. C. Li, Q. Huang, T. E. Mallouk, D. Wang, *J. Am. Chem. Soc.*, 2017, **139**, 15288-15291.

4 N. W. Li, Y. Shi, Y. X. Yin, X. X. Zeng, J. Y. Li, C. J. Li, L. J. Wan, R. Wen, Y. G. Guo, *Angew. Chem. Int. Ed. Engl.*, 2018, **57**, 1505-1509.

5 W. Tang, X. S. Yin, Z. X. Chen, W. Fu, K. P. Loh, G. W. Zheng, *Energy Storage Mater.*, 2018, **14**, 289-296.

6 Q. Li, S. P. Zhu, Y. Y. Lu, *Adv. Funct. Mater.*, 2017, **27**, 1606422.

7 Q. Song, H. Yan, K. Liu, K. Xie, W. Li, W. Gai, G. Chen, H. Li, C. Shen, Q. Fu, S. Zhang, L. Zhang, B. Wei, *Adv. Energy Mater.*, 2018, **8**, 1800564.

8 H. Zhao, D. N. Lei, Y. B. He, Y. F. Yuan, Q. B. Yun, B. Ni, W. Lv, B. H. Li, Q. H. Yang, F. Y. Kang, J. Lu, *Adv. Energy Mater.*, 2018, **8**, 1800266.

9 C. Yang, Y. Yao, S. He, H. Xie, E. Hitz, L. Hu, *Adv. Mater.*, 2017, **29**, 1702714.

10 D. Wang, C. Luan, W. Zhang, X. Liu, L. Sun, Q. Liang, T. Qin, Z. Zhao, Y. Zhou, P. Wang, W. Zheng, *Adv. Energy Mater.*, 2018, **8**, 1800650.

11 Y. Wang, Z. Wang, D. Lei, W. Lv, Q. Zhao, B. Ni, Y. Liu, B. Li, F. Kang, Y. B. He, *ACS Appl. Mater. Interfaces*, **2018**, 10, 20244-20249.

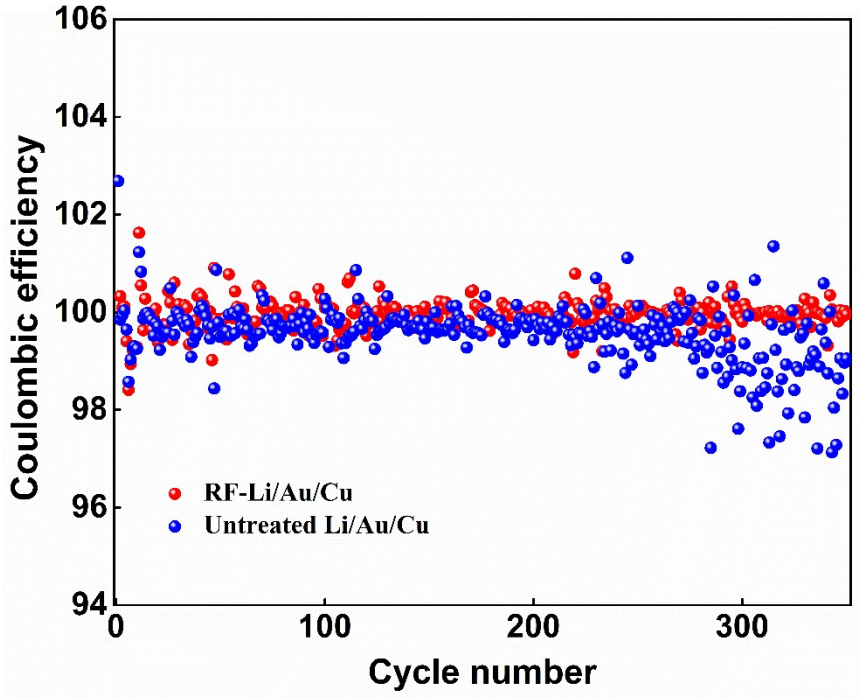

Fig. S13† Coulombic efficiency of $LiFePO_4$ full cells with RF-Li/Au/Cu and untreated Li/Au/Cu electrodes at 1 C rate.

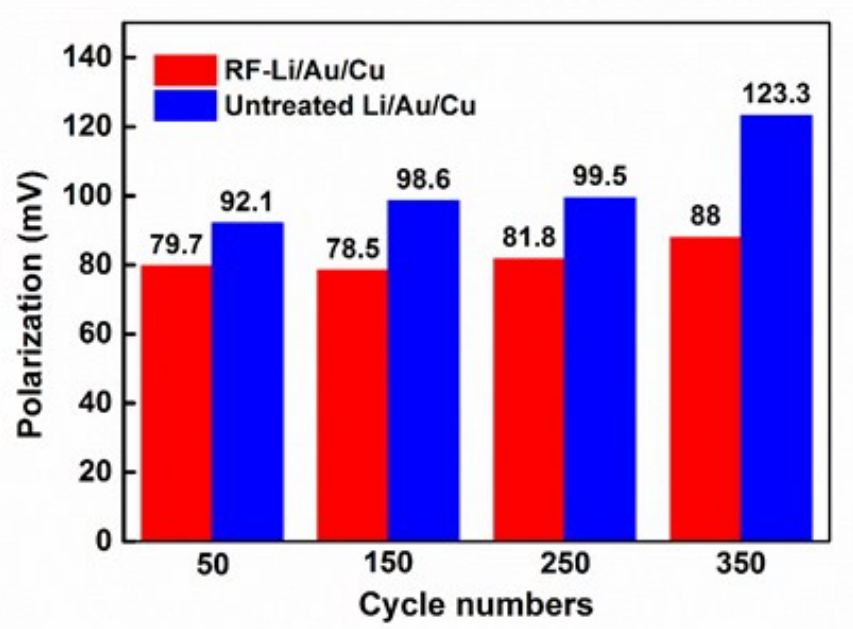

Fig. S14† Polarization comparison of $LiFePO_4$ full cells with untreated Li/Au/Cu and RF-Li/Au/Cu electrodes.